Colloidal Sphere Formation, H-Aggregation, and Photoresponsive Properties of an Amphiphilic Random Copolymer Bearing Branched Azo Side Chains

Yonghong Deng, Yaobang Li, and Xiaogong Wang*

Department of Chemical Engineering, Laboratory for Advanced Materials, Tsinghua University, Beijing, P. R. China 100084

Received June 15, 2006; Revised Manuscript Received July 21, 2006

ABSTRACT: This work studied the colloidal sphere formation, H-aggregation, and photoresponsive properties of an amphiphilic random copolymer functionalized with branched azo side chains ($POAPB_6P$-AC). The colloidal spheres were prepared through gradual hydrophobic association of the polymer chains in THF−H_2O media, which was induced by a continuous increase in the water content. The forming process and morphology of the colloidal spheres were characterized by DLS, SLS, and TEM. UV−vis spectroscopy was used to study the azo chromophore H-aggregation and structure variation in the colloid formation process by measuring the parameters such as λ_{max}, the trans-to-cis photoisomerization rate, and the isomerization degree at the photostationary state. The results indicate that the colloidal sphere formation undergoes several different stages as the water content increases. The polymeric chains start to associate at the critical water content (CWC). CWC is related with the initial concentration of the polymer in THF and is estimated to be 23 vol % when the initial concentration is 1.0 mg/mL. When the water content increases beyond the CWC, more and more polymer chains change from "isolated" single chains to clusters of associated chains. When the water content reaches 37%, almost all polymer chains are involved in the clusters. As the water content further increases, the clusters experience a collapse caused by the strong hydrophobic interaction, which is indicated by a dramatic size contraction detected from the DLS measurements. When the water content reaches about 60 vol %, the azo chromophores of $POAPB_6P$-AC start to form H-aggregates, which is indicated by a significant blue shift (from 360 to 339 nm) of the UV−vis maximum absorption band. The structure variation can also be detected from the photoisomerization behavior of the systems. When the water content changes from 50 to 60 vol %, both the trans-to-cis photoisomerization rate and the isomerization degree at the photostationary state decrease dramatically. Finally, when the water content increases from 95 to 100 vol %, the isomerization rate and degree significantly decrease again. In this stage, THF in the microphase is almost completely replaced by H_2O, and colloidal structure is "frozen" because of the free volume decrease and chain entanglement. The above observations give insight into the occurrence of H-aggregation in colloids of amphiphilic azo polymers for the first time. The understanding can lead to further development in expanding functionalities of the photoresponsive colloidal spheres through manipulation of the chromophore aggregation.

1. Introduction

Polymers containing aromatic azo chromophores (azo polymers for short) have received considerable attention in recent years.[1−4] Upon light irradiation, azo polymers can show a variety of structure and property variations triggered by the trans−cis photoisomerization of the azo chromophores. For instance, depending on the polymeric architectures and condensation states, the photoresponsive variations can behave as phase transition,[5] anisotropic chromophore orientation,[6] surface relief gratings,[7,8] and film contraction or bending.[9−11] Polymers with such properties are promising in the applications such as photoswitching, optical data-storage, sensors, light-driven reactors, and artificial muscles.[10,12−14] Recent research has shown that, by incorporation of ionizable groups in the structural units or segments, those interesting properties of azo polymers can be further extended to new areas of material design and preparation.[15−21] The photoresponsive materials with nano/micrometer dimensions can be prepared through methods such as electrostatic layer-by-layer (ELBL) deposition and hydrophilic-and-hydrophobic association in selective solvents.[22,23] Electrostatic multilayer films have been prepared through sequential deposition in solutions of an azo polyelectrolyte and an opposite-charged polyion.[15−17,19,20] The multilayer films can exhibit interesting properties such as significant second-order optical nonlinearity without electric field poling,[15−17] photochromic effect and photoinduced wettability change.[19,20] Photodeaggregatable micelles have been prepared through intermolecular association of a block azo copolymer in the selective solvent.[21] To further explore those photoresponsive materials through self-assembling approaches, a better understanding of the different interactions existing in the systems and their influence on the structure formation is required.

Besides the electrostatic and hydrophobic interactions generally observed in ELBL multilayers and micelle-like aggregates, there is a unique type of strong van der Waals interaction existing between conjugated planar structures.[24] The $\pi-\pi$ interaction can cause the organic compounds possessing such structures to form molecular aggregates with close intermolecular spacing and strong coupling. Early studies indicated that ionic dyes could form different dye−dye aggregates and show metachromacy in aqueous or mixed aqueous−organic solutions.[25,26] Because of those early stage investigations, the $\pi-\pi$ aggregation has been named according to the relative position of the aggregate absorption band to the molecular absorption band (M-band). H-aggregation denotes the aggregation showing a blue-shifted band (hypsochromic band or H-band) to the M-band and J-aggregation (after Jelley and Scheibe) refers to the aggregation exhibiting a red-shifted band and resonance

* Corresponding author: e-mail wxg-dce@mail.tsinghua.edu.cn.

10.1021/ma061335p CCC: $33.50
Published on Web 08/23/2006

fluorescence.[25,26] The large spectral shifts and distinct changes in band shapes can be rationalized on the basis of the exciton model and screening model.[27,28] As the dye−dye aggregation is accompanied by significant color and luminescence variations, the aggregation and its effect have been intensively investigated in the fields of photographic science and engineering,[25,26] textile coloring,[29] biophotonics,[30] and linear and nonlinear optics.[31] Azo chromophores can form $\pi-\pi$ aggregates under different conditions. As the their transition dipole moments are usually parallel to the long axis of the molecules, azo chromophores take H-aggregation as the typical aggregation manner.[29,32−35] H-aggregation of azo chromophores has been observed in systems such as monolayers, bilayers, LB films, membranes, and vesicles.[32] H-aggregation of azobenzene phospholipids in bilayers has been studied and used to prepare photoregulatable membrane and related materials.[33] On the other hand, it has been reported that H-aggregation cannot be observed in spherical micelles containing azobenzene surfactants because the packing is too loose and the chromophores cannot adopt the required configuration in the micelles.[34] For ELBL self-assembly of bolaamphiphiles or polyelectrolytes containing azobenzene units, H-aggregation is often observed in the dipping solutions.[35]

In our previous works, a series of amphiphilic azo homopolymers and random copolymers were synthesized and used to construct the uniform photoresponsive colloidal spheres.[36−39] The colloidal spheres were prepared through gradual hydrophobic aggregation of the polymeric chains in mixed aqueous−organic dispersion media, induced by a continuous increase in the water content. The colloidal spheres possess some interesting properties such as shape deformation and dichroism upon light irradiation.[36,37] The colloidal spheres can be used to prepare two-dimensional colloidal arrays and ordered mesoporous films through in-situ structure inversion.[37,38] The photoisomerization of azo chromophores in the colloids depends on the preparation conditions, which influence the structure of the colloidal spheres.[39] In another separate study, a polyelectrolyte functionalized with branched side chains bearing the pseudo-stilbene-type azo chromophores was used as the polyanion to build up multilayer films through ELBL adsorption by using poly(diallyldimethylammonium chloride) (PDAC) as the polycation.[40] During this process, H-aggregation of azo chromophores was detected to occur both in the dipping solutions and in the corresponding multilayers. When the H-aggregation degree was adjusted by the ratio of the organic solvent to water in the dipping solutions, the structure and properties of the ELBL multilayers could be significantly modified by the solution conditions. Although it has been known that H-aggregation can cause the intermolecular and intramolecular association in aqueous solutions, its effect on the colloidal formation and properties has not been studied in those early phase studies. Therefore, it is unclear whether H-aggregation can play an important role to influence the structure and properties of those photoresponsive colloids.

In the current work, a new poly(acrylic acid)-based amphiphilic polymer ($POAPB_6P$-AC) was synthesized and used to assemble photoresponsive colloidal spheres through the gradual hydrophobic aggregation scheme. $POAPB_6P$-AC was designed to have branched side chains bearing the azobenzene-type chromophores, which can form H-aggregates in mixed aqueous−organic solvents. As the azobenzene-type chromophores have a relatively stable cis form, the photoisomerization can be feasibly monitored by UV−vis spectroscopy.[41] The measured isomerization rate and degree are closely related with the microenvironment around the chromophores.[1,39,41] On the basis of the polymer, the colloidal spheres were prepared and the formation of the colloids was characterized by the static light scattering (SLS), dynamic light scattering (DLS), and transmission electron microscopy (TEM). H-aggregation of azo chromophores occurring in the colloid formation process was investigated by UV−vis spectroscopy. The isomerization behavior was studied and used as a probe to detect the microenvironmental variation in the process. Results indicate that as the water content increases, the colloidal sphere formation undergoes several different stages such as polymeric chain association, the cluster collapse, and the structure "freeze". In the process, only when the water content reaches a relatively high value and the clusters undergo a significant size contraction do the azo chromophores of $POAPB_6P$-AC start to form H-aggregates. The H-aggregation is closely related with the structure variation occurring during the colloid formation process and shows a significant influence on the photoisomerization behavior of the azo chromophores.

2. Experimental Section

Characterization. ^1H NMR spectra were obtained on both Bruker AM-500 (500 MHz for proton) and Varian Unity-200 (200 MHz for proton) FT-NMR spectrometers. IR spectra were determined on a Nicolet 560-IR FT-IR spectrophotometer by incorporating the powder samples in KBr disks. Elemental analyses (EA) of C, H, and N were measured by the Heratus CHN-Rapid method. The melting points of azo compounds and T_g of the polymer were determined with a TA Instruments DSC 2910 at a heating rate of 10 °C/min. The UV−vis spectra of the samples were recorded by using an Agilent 8453 UV−vis spectrophotometer. The molecular weights and their distributions of the polymers were determined by gel permeation chromatography (GPC) utilizing a Waters model 515 pump and a model 2410 differential refractometer with three Styragel columns HT2, HT3, and HT4 connected in a serial fashion. THF was used as the eluent at a flow rate of 1.0 mL/min. Polystyrene standards with dispersity of 1.08−1.12 obtained from Waters were employed to calibrate the instrument. TEM images of the colloidal spheres were obtained by using a JEOL-JEM-1200EX electron microscope with an accelerating voltage of 120 kV. The TEM samples were prepared by dropping diluted sphere dispersions onto the copper grids coated with a thin polymer film and then dried in a 30 °C vacuum oven for 24 h. No staining treatment was performed for the measurements. Static light scattering (SLS) and dynamic light scattering (DLS) experiments were performed on a DLS-7000 multiangle laser photometer (OTSUKA Instruments Corp.) equipped with a He−Ne laser (632.8 nm). The derivative refractive index increment value (dn/dC) was measured by an OTSUKA Rm-102 differential refractometer. The four solutions with different concentrations used in Zimm plot processing were obtained by dilution of a more concentrated original solution. To ensure that SLS and DLS measurements were not affected by dust, the stock solutions were filtered twice through membrane filters with normal pore size of 0.45 μm, transferred to dust-free glassware, and then diluted with the filtered solvents. All the experiments were performed at 25 °C over a range of concentrations and detection angles. The size and size distribution of the colloidal spheres were also measured with a Marvern Zetasizer 3000 dynamic light scattering instrument equipped with a multi-τ digital time correlator and a 632.8 nm solid-state laser light source. The scattering angle used for the measurement was 90°, and the sample temperature was controlled to be 25 °C.

Materials. Analytical pure tetrahydrofuran (THF) from commercial source was refluxed with cuprous chloride and distilled for dehydration before use. Deionized water (resistivity >18 MΩ·cm) was obtained from a Millipore water purification system and used for the following experiments. Other reagents and solvents were used as received without further purification.

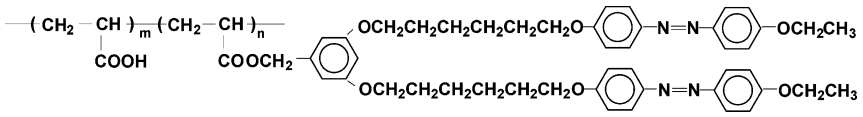

Figure 1. Chemical structure of $POAPB_6P$-AC.

Synthesis of $POAPB_6P$-AC. The chemical structure of $POAPB_6P$-AC is given in Figure 1. $POAPB_6P$-AC is a random copolymer composed of hydrophilic ionizable carboxyl groups and hydrophobic branched azo side chains. $POAPB_6P$-AC was prepared by the Schotten−Baumann reaction between poly(acryloyl chloride) (PAC) and 3,5-bis{6-[4-(4′-ethoxyphenylazo)phenoxy]hexyloxy}benzyl alcohol ($OAPB_6P$). After the reaction, the unreacted acyl chloride groups were hydrolyzed to obtain the carboxyl groups. PAC was prepared by the radical polymerization of acryloyl chloride as reported in our previous paper.[42] The scheme for synthesis of $OAPB_6P$ and $POAPB_6P$-AC is given in Scheme S1 (in the Supporting Information). The analytical data and spectra of products of each step reaction for $OAPB_6P$ synthesis are also given in the Supporting Information. The reaction between PAC and $OAPB_6P$ was carried out according to the conditions reported previously.[42] As it was difficult to directly measure the molecular weight and its distribution of PAC due to the high reactivity of acyl chloride groups, a gel permeation chromatography (GPC) measurement was carried out on a poly(methyl acrylate) sample that was prepared by the reaction between the same-batch synthesized PAC and excess methanol.[42] The number-average molecular weight of PAC estimated by the result of the poly(methyl acrylate) sample was 21 600 with a polydispersity index of 1.53. The degree of functionalization (DF) of $POAPB_6P$-AC is defined as the percentage of the structure units bearing azo chromophores among the total structure units. DF was controlled by selecting a suitable feed ratio between PAC and $OAPB_6P$. For POAPB6P-AC sample used in this work, DF estimated by the elemental analysis was 14.5%. The weight-average molecular mass ($M_{w,m}$) of the $POAPB_6P$-AC sample was obtained from the static light scattering measurement. The dn/dC value of $POAPB_6P$-AC in THF solution was measured to be 0.165, and $M_{w,m}$ was estimated to be 100 900 from the Zimm plot. The other analytical data of $POAPB_6P$-AC are given as follows. ^{1}H NMR (DMSO-d_6), δ: 12.40, 7.80, 7.00, 6.60, 6.45, 4.97, 4.32, 3.99, 2.25, 1.81, 1.35. IR (KBr, cm^{-1}): 3600−3200 (COOH, br), 2921 and 2861 (CH_2, str), 1725 (C═O, str), 1600 1580 1500 (benzene ring, str), 1250 (C−O, str). EA: 4.42 (N), 65.33 (C); 6.55 (H); T_g: 154 °C; UV−vis (THF): λ_{max} = 360 nm.

Sample Preparation. Suitable amounts of $POAPB_6P$-AC were dissolved in THF to obtain solutions with different initial concentrations (0.03−1.0 mg/mL). The initial concentrations mentioned in the following text refer to the initial concentrations of $POAPB_6P$-AC in THF. An initial concentration of 1.0 mg/mL was used for most experiments in this work, except those specifically designed to study the effect of the initial concentration. The solutions were kept stirring for 20 min and then put aside for 72 h. To obtain solutions or dispersions of $POAPB_6P$-AC in THF−H_2O media with different water contents, the required amounts of water were added into the stirred THF solutions at a rate of 5 μL/s. After the water addition was completed, the solutions or dispersions were left to equilibrate for at least 24 h. The light scattering measurement was preformed on the solutions or dispersions to determine the parameters such as the critical water content (CWC) and the hydrodynamic radius (R_h). For preparation of the stable colloidal dispersions, water was added into the THF solution in a similar manner as mentioned above until the water content reached 70 vol %, and then the dispersion was "quenched" by adding excess water and dialyzed against water for 72 h to remove THF.

Photoisomerization Study. The photoisomerization of the azo chromophores was induced by irradiation with UV light, which was from a high-intensity 365 nm UV lamp equipped with 12.7 cm diameter filter (Cole-Parmer L-97600-05 long wave UV lamp, U-09819-23 filter). The light intensity of the lamp was 7000 mW/cm^2 at a distance of 38 cm and 21 000 mW/cm^2 at a distance of 5 cm. The samples were placed at ca. 15 cm away from the lamp. The surrounding temperature of the samples was controlled to be about 30 °C by a cold plate. The UV−vis spectra of the samples were measured over different irradiation time intervals by using an Agilent 8453 UV−vis spectrophotometer. To study the effect of the water content on photoresponsive behavior, the $POAPB_6P$-AC solutions or dispersions with different water contents were irradiated with the 365 nm UV light, and the UV−vis spectra were recorded over different time intervals until the photostationary states were achieved. For measuring the thermal cis-to-trans isomerization, the samples were kept in a dark oven with constant temperature (30 ± 1 °C), and the UV−vis spectra were recorded over different time intervals.

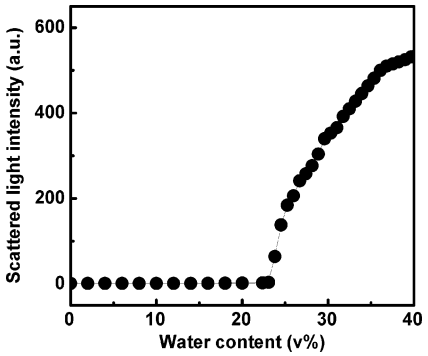

Figure 2. Scattering light intensity as a function of the water content (vol %) in the THF−H_2O dispersion media. The initial concentration of $POAPB_6P$-AC in THF was 1.0 mg/mL.

3. Results and Discussion

The chemical structure of $POAPB_6P$-AC is given in Figure 1. $POAPB_6P$-AC is an amphiphilic random copolymer composed of hydrophilic acrylic acid units and hydrophobic branched azo side-chain units. The degree of functionalization (DF) is 14.5% for the sample used in this work. Because of the preparation method, $POAPB_6P$-AC possesses polydispersity in composition, sequence distribution, and molecular weight. The polymer could be dissolved in anhydrous THF to form homogeneous solutions with different concentrations and could form colloidal spheres through a stepwise buildup process when water was gradually added into the solutions. The details of the colloid formation and its relationship with H-aggregation and photoresponsive properties will be presented and discussed in the following sections.

3.1. Critical Water Content (CWC) for Chain Association. When water was gradually added into the THF solutions, $POAPB_6P$-AC chains started to associate with each other in the solutions due to the hydrophobic interaction, which was reflected in an abrupt increase in the scattered light intensity. Like the study of amphiphilic block copolymers,[43] the critical water content (CWC) is defined as the water content at which the polymer chains start to associate. CWC was obtained from the turning-up point on the plots of the light scattering intensity vs the water content in the medium. Figure 2 presents a typical plot, where the initial concentration of $POAPB_6P$-AC in THF is 1.0 mg/mL. The diagram shows that a jump in scattered light intensity occurs at the water content of 23 vol %, which corresponds to the critical water content of the $POAPB_6P$-AC solution.

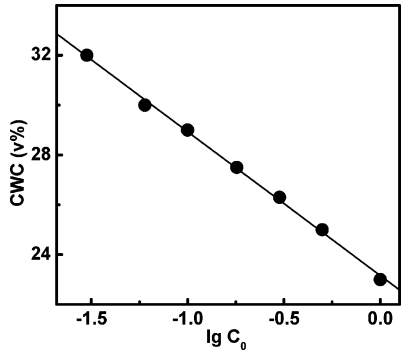

Figure 3. Plot of the critical water content (CWC) vs logarithm of the initial concentration (C_0) of $POAPB_6P$-AC in THF.

For amphiphilic block copolymers, CWC depends on both the initial polymer concentration and the molecular weight of the polymer.[43a] The higher the initial polymer concentration or the molecular weight, the lower is the CWC value. A similar tendency has been observed for amphiphilic random azo copolymers.[37,39] For $POAPB_6P$-AC, the same tendency was also observed (Figure 3). A linear inverse proportion relationship exists between CWC and the logarithm of the initial polymer concentration (C_0).

3.2. Influence of the Water Content on Chain Association Fraction. When the water content increases beyond CWC, more and more polymer chains associate to form clusters, and consequently the concentration of "isolated" single chains in the solution decreases gradually. The change of the fraction of the associated chains as a function of the water content can be estimated by using the method proposed by Eisenberg et al. to calculate the micelle fraction of amphiphilic block copolymers.[43a]

As shown in Figure 3, the relationship between CWC and the initial polymer concentration C_0 can be expressed as

$$\mathrm{CWC} = -A \log C_0 + B \tag{1}$$

$$C_0 = \exp[2.303(B - \mathrm{CWC})/A] \tag{2}$$

where A and B are two constants and need to be determined for a specific polymer system. At the critical water content, the polymer concentration represents essentially the critical polymer concentration (CPC) for colloid formation, which depends on the molecular weight of the polymer and the water content. For $POAPB_6P$-AC with a specific molecular weight, the higher the water content, the lower is CPC. CPC mentioned here also corresponds to the concentration of the unassociated polymer chains in the solution (C_{unass}). When the added water increases gradually, more and more polymer chains form clusters of associated chains. However, the concentration of the unassociated polymer chains still obeys a relationship similar to eq 1. Therefore, a similar equation as eq 2 can be obtained

$$C_{\mathrm{unass}} = \exp[2.303(B - C_{\mathrm{w}})/A] \tag{3}$$

where C_{w} represents the water content (vol %) in the solution.

The fraction of the associated polymeric chains among the total can be calculated by $(C_0 - C_{\mathrm{unass}})/C_0$. By combining eqs 2 and 3, the following relationship can be obtained:

$$(C_0 - C_{\mathrm{unass}})/C_0 = 1 - \exp[2.303(\mathrm{CWC} - C_{\mathrm{w}})/A]$$
$$= 1 - \exp(-2.303\Delta H_2O/A) \tag{4}$$

where ΔH_2O represents the increment of added water above CWC, which is also given as the volume percentage.

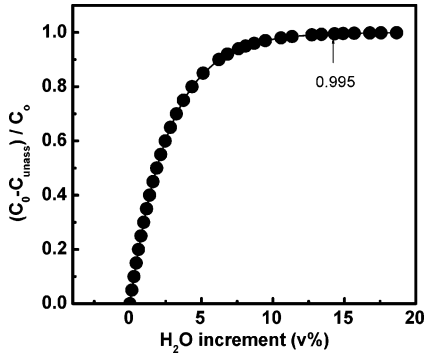

Figure 4. Fraction of the associated chains as a function of the water increment beyond CWC. Arrow indicates the water content where 99.5% chains are involved in the clusters.

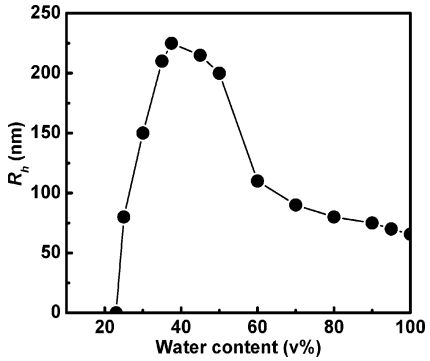

Figure 5. Relationship between the average hydrodynamic radius (R_{h}) of the structures formed in the H_2O−THF media and the water content. The initial concentration of $POAPB_6P$-AC in THF was 1.0 mg/mL.

The constant A, whose value depends on specific polymer and organic solvent, can be obtained from the slope of the plot of CWC vs log C_0 (Figure 3). By using eq 4, the change of $(C_0 - C_{\mathrm{unass}})/C_0$ as a function of the H_2O increment can be calculated. A plot of $(C_0 - C_{\mathrm{unass}})/C_0$ against the H_2O increment is shown in Figure 4, where the initial polymer concentration is 1.0 mg/mL and CWC is 23 vol %. When ΔH_2O is 14 vol % (i.e., the water content is 37%), the percentage of polymer chains involved in the clusters of the associated chains is calculated to be 99.5%. Therefore, over the water content, the amount of the "isolated" single chains in the solution is negligible. Comparing with amphiphilic block copolymer,[43a] ΔH_2O is much larger, which indicates that as the water content increases, the transition of $POAPB_6P$-AC molecules from "isolated" single-chains to associated chains is a gradual process.

3.3. Influence of the Water Content on Colloid Formation. When the water content further increases, the $POAPB_6P$-AC chains can finally form colloidal spheres in the dispersions. The colloid formation through chain association is a complicated process. In the process, the polymer chains undergo transition from dilute polymer solution, through semidilute state, to the densely packed state before colloid formation. Although it is difficult to specify the structural details in the colloid formation process, light scattering study can give some useful information about the transition process. For consistency, the initial polymer concentration of 1.0 mg/mL is used as a typical condition for all the following discussions. Figure 5 shows the hydrodynamic radius (R_{h}) of the structures forming in the dispersions with different water contents, which was measured by dynamic light scattering (DLS). When the water content increases in the range from 23 to 37 vol %, R_{h} correspondingly increases with the water content increase because more and more chains associate to form the clusters. When the water content increases from 37

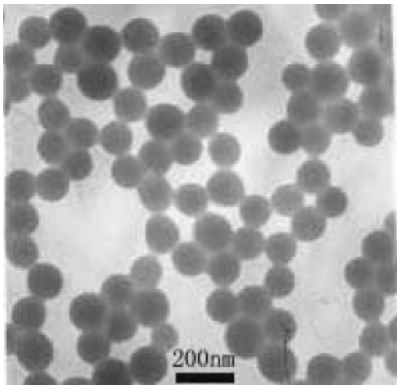

Figure 6. Typical TEM image of the colloidal spheres obtained from the aqueous dispersion. The initial concentration of $POAPB_6P$-AC in THF was 1.0 mg/mL.

to 60 vol %, R_h decreases dramatically, which corresponds to the cluster collapse induced by hydrophobic interaction. When the water content increase over 60 vol %, R_h starts to decrease slowly as the water content further increases. After this stage, SEM and TEM observations indicate that uniform colloidal spheres can be obtained by "quenching" the structures in dispersions with excess water. The 60% water content is a turning point. Before this point, the structures formed in the dispersions are believed to be loose clusters having irregular shape and fracton dimensionality. Therefore, when the water content is in the range from 23 to 60 vol %, the R_h estimated from DLS by using the Stokes−Einstein relation can only be treated as semiquantitative values. The spectroscopic study given in the following sections can further confirm that the structures forming in the water content range have characteristics of loose clusters.

3.4. Characterization of Colloidal Spheres. When the water contents are higher than 60%, stable aqueous dispersions of $POAPB_6P$-AC colloids can be obtained by adding an excessive amount of water to "quench" the structures formed in the dispersions and then dialyzing against water to remove THF. Figure 6 shows a typical TEM image of the colloids separated from the stable colloid dispersion. It shows that uniform colloidal spheres form under the condition. The average size of the spheres was estimated to be 120 nm, obtained from the statistics of 100 contiguous spheres in the TEM images.

The DLS was used to determine the average hydrodynamic radius (R_h) and polydispersity of colloidal spheres in the aqueous dispersion medium. For estimating those parameters, the cumulant method was used to describe logarithm of the total autocorrelation function as a series expansion, where the first cumulant (Γ) yields the *z*-averaged diffusion coefficient and the second cumulant (μ_2) is a measure of polydispersity.[44a] R_h was obtained from the particle diffusion coefficient based on the Stokes−Einstein relation.[44b] Figure 7 shows the size distribution curve obtained from the DLS measurement. The *z*-averaged hydrodynamic radius (R_h) is 65.6 nm with the polydispersity (μ_2/Γ^2) of 0.025.

The static light scattering (SLS) was used to determine the weight-average mass of the colloidal particles ($M_{w,p}$), the radius of gyration (R_g), and the second virial coefficient (A_2).[45] According to the basic SLS theory, the particles scatter light according to the following relation:

$$\frac{KC}{R(\theta)} = \frac{1}{M_{w,p}}\left(1 + \frac{16\pi^2 n^2 \sin^2\left(\frac{\theta}{2}\right)\langle R_g^2\rangle}{3\lambda_0^2}\right) + 2A_2C \qquad (5)$$

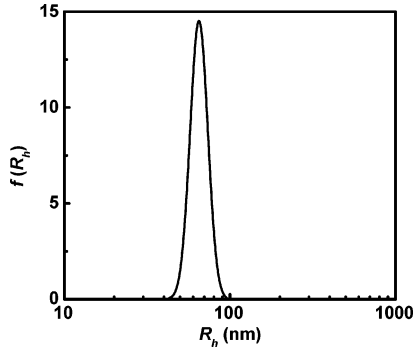

Figure 7. Distribution of the hydrodynamic radius (R_h) of the $POAPB_6P$-AC colloidal spheres in the aqueous dispersion. The initial polymer concentration in THF was 1.0 mg/mL.

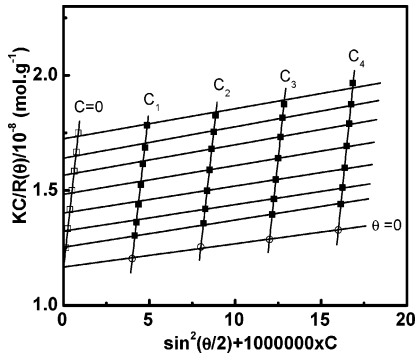

Figure 8. Static Zimm plot of the $POAPB_6P$-AC colloid spheres in the water dispersion. The spheres were prepared from a THF solution with an initial polymer concentration of 1.0 mg/mL. The four concentrations of the $POAPB_6P$-AC colloidal dispersions were $C_1 = 4 \times 10^{-6}$ g/mL, $C_2 = 8 \times 10^{-6}$ g/mL, $C_3 = 1.2 \times 10^{-5}$ g/mL, and $C_4 = 1.6 \times 10^{-5}$ g/mL.

Table 1. DLS and SLS Experimental Results for the Colloidal Spheres Dispersed in Water[a]

R_h (nm)	μ_2/Γ^2	R_g (nm)	R_g/R_h	A_2	$M_{w,p}$ (g/mol)	N_{agg}[b]	ρ[c] (g/cm^3)
65.6	0.025	50.8	0.774	5.05×10^{-5}	8.62×10^7	854	0.121

[a] Here μ_2/Γ^2 is the polydispersity index of the spheres dispersed in the water, measured by DLS. The d*n*/d*C* value of the colloidal dispersion was measured to be 0.255. [b] $N_{agg} = M_{w,p}/M_{w,m}$. [c] $\rho = M_{w,p}/(N_A 4\pi\langle R_h\rangle^3/3)$.

where *K* is the contrast factor, *C* is the concentration, θ is the angle at which scattering light is measured, $R(\theta)$ is the Rayleigh ratio at the angle of measurement, *n* is the refractive index of the solvent, λ_0 is the wavelength of the incident light, and A_2 is the second virial coefficient. The parameters were estimated through the Zimm plot analysis (Figure 8). The extrapolations regarding to *C* and θ yield $M_{w,p}$ from the intercept on the ordinate as well as A_2 and $\langle R_g^2\rangle$ from the slope of the corresponding curves. $M_{w,p}$, R_g, and A_2 obtained from Figure 8 are 8.62×10^7 g/mol, 50.8 nm, and 5.05×10^{-5}, respectively.

Table 1 summarizes the R_h, R_g, R_g/R_h, $M_{w,p}$, N_{agg}, and ρ values of the $POAPB_6P$-AC colloidal spheres. The R_g/R_h value can be used to characterize the shape of the colloids.[46] R_g/R_h estimated for the above sample is around 0.774, which confirms that the $POAPB_6P$-AC colloids are spherical particles in the suspension. The average aggregate number in each colloidal particle is estimated to be 854, based on the equation

$$N_{agg} = M_{w,p}/M_{w,m} \qquad (6)$$

where $M_{w,p}$ and $M_{w,m}$ are the weight-average mass of the colloidal particles and the polymeric molecules, respectively.[47,48]

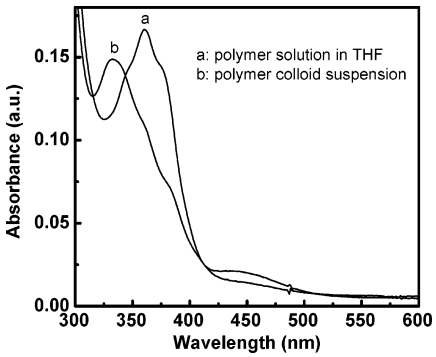

Figure 9. (a) UV−vis spectrum of $POAPB_6P$-AC in THF solution (5 mg/L). (b) UV−vis spectrum of $POAPB_6P$-AC colloids in the aqueous dispersion, which was prepared from the dispersion with the water content of 70 vol % through the "quenching" and dialyzing procedure, and the initial polymer concentration in THF was 1.0 mg/mL.

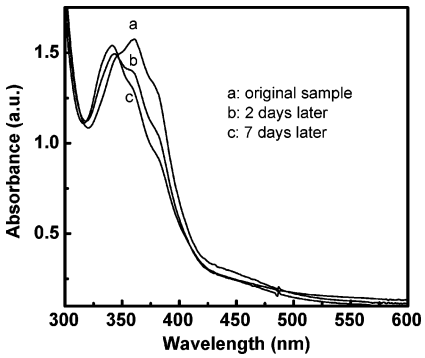

Figure 10. UV−vis spectra of $POAPB_6P$-AC colloids in the dispersion (0.04 mg/mL) measured for different storage periods: (a) right after water addition, (b) after 2 days, and (c) after 7 days. The colloidal dispersion was prepared by dropping water into the THF solution of $POAPB_6P$-AC until the water content reached 60 vol %; the initial polymer concentration in THF was 1.0 mg/mL.

The average density of the colloidal particles (ρ) is calculated to be 0.121 g/cm^3 by applying the following equation:[49]

$$\rho = M_{w,p}/(N_A 4\pi\langle R_h\rangle^3/3) \quad (7)$$

The above results all indicate that the structures formed in the aqueous dispersion are uniform colloidal spheres. The colloidal spheres of $POAPB_6P$-AC are stable in the dispersion medium because of the repulsive electrostatic interaction of the surface charges. No obvious variation was observed from the DLS measurement and the TEM observation after storing the colloidal dispersions at room temperature for months.

3.5. H-Aggregation of Azo Chromophores. The H-aggregation of azo chromophores of $POAPB_6P$-AC is closely related with the colloidal formation process, which can be monitored by spectroscopic analysis. Figure 9 gives UV−vis spectra of both $POAPB_6P$-AC dissolved in THF and $POAPB_6P$-AC colloids dispersed in water. $POAPB_6P$-AC in THF shows a maximum absorbance at 360 nm, corresponding to the $\pi-\pi^*$ transition of the "isolated" azo chromophores. For the aqueous dispersion of the colloidal spheres, the $\pi-\pi^*$ transition band shows a significant blue shift and appears at 334 nm. The blue shift is attributed to H-aggregation involving "card-packed" stacking of the azo chromophores.[25−27] The blue shift induced by H-aggregation can be distinguished from the band shifts caused by the solvatochromic effect. λ_{max} of $POAPB_6P$-AC in dioxane, THF, and DMF appears at 358, 360, and 362 nm, which indicates that the solvatochromic effect causes a red shift when polarity of the solvent increases, and the band shift is usually in a range of a few nanometers.

The transition from the "isolated" azo chromophores in THF solution to H-aggregates in the colloids is a process related with the water content increase in the system. UV−vis spectra measured in the process can be used to indicate the transition point of the H-aggregate formation. When the water content is low, UV−vis spectra of $POAPB_6P$-AC solutions or dispersions show the maximum absorption band at 360 ± 1 nm, which is almost the same as that of $POAPB_6P$-AC in THF. There is no significant band shift when the water content increases from 0% to a value below 60 vol %, which indicates that no significant H-aggregation occurs in the systems. When the water content reaches 60 vol %, the UV−vis spectrum of the dispersion changes significantly as the storage time increases. Figure 10 shows the UV−vis spectra of the colloidal dispersion with the water content of 60 vol % measured after different storage periods. For the spectrum measured right after the water addition, the spectral character is the same as that of the THF solution, where the maximum absorption band appears at 360 nm. When storing for 2 days, the UV−vis spectrum of the dispersion exhibits a broad absorption band with the peak at 340 nm and a shoulder at 360 nm, which indicates the coexistence of the "isolated" azo chromophores and H-aggregates of the chromophores. After storing for 7 days, the spectrum shows the maximum absorption band at 339 nm, which suggests that most of azo chromophores of $POAPB_6P$-AC form H-aggregates. When the water content further increases, λ_{max} of the $POAPB_6P$-AC dispersions changes from 360 to 339 nm in a shorter time period after the water addition. When the water content reaches 80%, the UV−vis spectrum of the dispersion shows the characteristics of H-aggregates immediately after the water addition. This indicates that under this condition the H-aggregates can be formed in an extremely short time period. Figure 11 shows that λ_{max} as a function of the water content in the solutions or dispersions, which were all measured after storing for 7 days. A sudden fall of λ_{max} in the diagram can be seen at the water content about 60 vol %. Over this water content, most of azo chromophores in the system form H-aggregates. In other words, azo chromophores of $POAPB_6P$-AC exist as "isolated" chromophores when water content is below 60 vol % and form H-aggregates when the water content is over this value. Comparing with the results given in section 3.3, it can be seen that H-aggregation occurs after the clusters undergo a significant size contraction. When water content reaches about 95 vol %, the λ_{max} again shows a blue shift from 339 to 334 nm. This transition is related with the structure "freeze", which will be discussed in the following section.

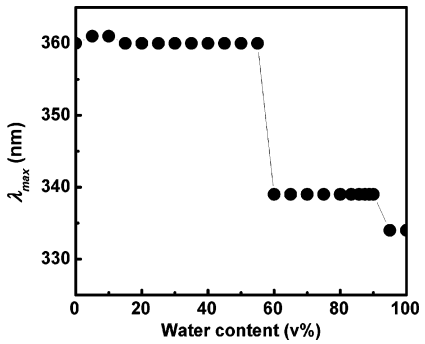

Figure 11. λ_{max} of the $\pi-\pi^*$ transition band of $POAPB_6P$-AC as a function of the water content in the mixed THF−H_2O media. The initial polymer concentration in THF was 1.0 mg/mL.

The above result can be rationalized on the basis of the following considerations. As the $\pi-\pi$ attraction is a short-range

interaction, H-aggregation can occur only when the chromophores can approach each other in space.[24−28] For low molecular weight compounds in solutions, the molecules can come close to each other through Brownian motion. In many cases, an equilibrium between "isolated" molecules and H-aggregates exists, which can be described by the mass action law.[25,26] In the current case, the azo chromophores are tethered on the polymeric chain, and their movement through Brownian motion is restricted by the backbone. Therefore, the azo chromophores can approach each other only when polymer chains are closely packed through the chain association and cluster collapse. This condition can be satisfied only when the water content in the system is relatively high, such as 60 vol % for the above case. Only in this high water content range can H-aggregation be observed in a reasonably short period of time. It has been reported that for ionic dyes H-aggregation can be directly promoted by the hydrophobic interactions.[26] For polymeric system discussed in this paper, the hydrophobic interaction shows a more complicated influence on the H-aggregation, which is closely related with the polymer conformation and association state in the dispersion media.

3.6. Photoisomerization Behavior. As the photoisomerization of azobenzene units is sensitive to the local environment surrounding the units, information about the local structure and its variation can be obtained by measuring the isomerization rate and the isomerization degree at the photostationary state.[1,39,42] In this work, the photoisomerization of the azobenzene units was investigated and used as a tool to probe the structure variations of $POAPB_6P$-AC in the different dispersion media.

Figure 12a−c shows the spectra corresponding to the photoisomerization of $POAPB_6P$-AC, which is dissolved in anhydrous THF, dispersed in the THF−H_2O medium with the water content of 60 vol %, and dispersed in the aqueous medium, respectively. The samples were irradiated with 365 nm UV light for different time periods, and the UV−vis spectra of the samples were recorded until the photostationary states were achieved. For $POAPB_6P$-AC dissolved in anhydrous THF (Figure 12a), the absorbance of the $\pi-\pi^*$ transition band at 360 nm gradually decreases, and the absorbance of the $n-\pi^*$ transition band at 450 nm gradually increases upon the light irradiation. The spectral variations evidence the trans-to-cis isomerization of the azobenzene-type chromophores.[1,41] When the sample was kept in a dark oven, the spectra gradually recovered the original curve, where the azo chromophores underwent a slow thermal cis-to-trans isomerization. For the $POAPB_6P$-AC dispersion with the water content of 60 vol % (Figure 12b) and the aqueous colloidal dispersion (Figure 12c), λ_{max} before light irradiation appears at 339 and 334 nm because of H-aggregation and the "frozen" structure. Upon the light irradiation, those systems can also show obvious trans-to-cis isomerization. However, it can be seen that the photoinduced spectral variations show different characteristics. From Figure 12a−c, the absorbance at λ_{max} before the light irradiation (A_{origin}) and the absorbance at the same wavelength after the irradiation for different time periods (A_t) can be obtained. The relative absorbance (A_t/A_{origin}) of the samples can be used to indicate the relative amount of the trans isomers remaining at t time. The variations of A_t/A_{origin} with t represent the kinetics of the photoisomerization. For Figure 12a−c, the variations can be best fitted by the first-order exponential decay function

$$A_t/A_{origin} = A_0 + A_1 \exp(-t/T_1) \quad (8)$$

where T_1 is the characteristic time of the decay process. Both experimental data and fitting curves are shown in the insets of Figure 12a−c. T_1 obtained from the curve fitting is 5.4, 27.3, and 33.7 s for parts a, b, and c of Figure 12. Comparing with the THF solution, the trans-to-cis isomerization rate declines significantly for the dispersion given in Figure 12b. For the aqueous colloidal dispersion (Figure 12c), the isomerization rate shows an even further decrease.

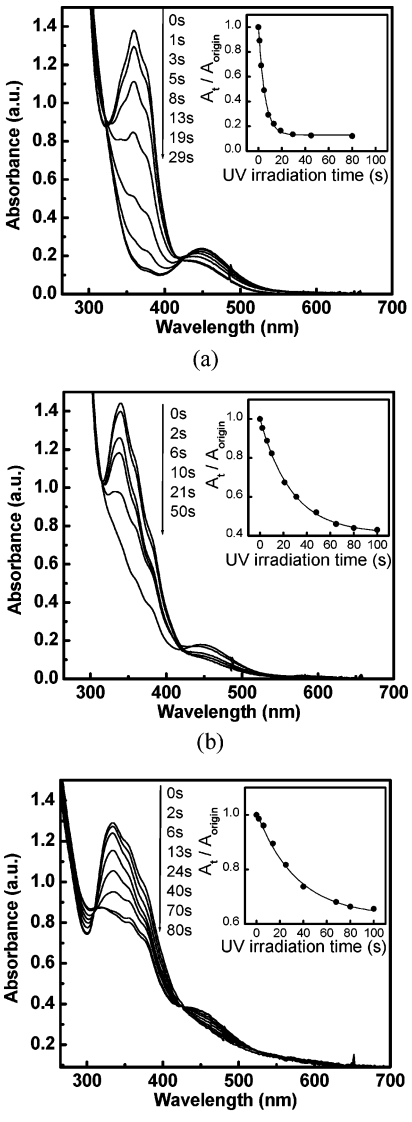

Figure 12. Variation of the UV−vis spectra of $POAPB_6P$-AC in different media induced by the UV light irradiation. Inset: the relative absorbance (A_t/A_{origin}) varying with the irradiation time and the fitting curves. (a) $POAPB_6P$-AC dissolved in THF solution (0.033 mg/mL); (b) $POAPB_6P$-AC dispersed in the mixed THF−H_2O media (0.035 mg/mL) with the water content of 60 vol %; (c) $POAPB_6P$-AC dispersed in water (0.035 mg/mL). The initial polymer concentrations in THF were all 1.0 mg/mL.

For the other solutions or dispersions of $POAPB_6P$-AC in THF−H_2O media with different water contents, the photoisomerization processes were studied in the same way. Figure 13a shows the relative absorbance (A_t/A_{origin}) of the samples varied with the UV light irradiation time period. For all the samples, the variations of A_t/A_{origin} with the irradiation time can be best fitted by the first-order exponential decay function. Both the experimental data and fitting curves are shown in Figure 13a, and the parameters obtained from the fitting are given in Table 2. The results indicate that the trans-to-cis isomerization rate is closely related with the water content in the system. When the water content changes from 0% (THF solution) to 23 vol

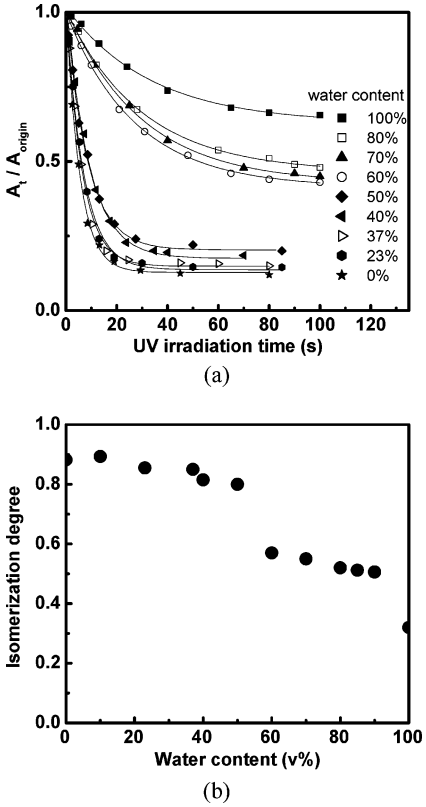

Figure 13. (a) Plot of the relative absorbance (A_t/A_{origin}) of $POAPB_6P$-AC in various media vs the irradiation time period. (b) Plot of the photoisomerization degree at the photostationary state vs the water content in the dispersion media.

Table 2. Parameters of the Photoisomerization Kinetics Obtained from the Curve Fitting for $POAPB_6P$-AC Dissolved or Dispersed in THF−H_2O Media with Different Water Contents[a]

sample (water content, %)	A_0	A_1	T_1 (s)	χ^2
0	0.12	0.88	5.45	2.87×10^{-4}
23	0.14	0.88	6.29	4.29×10^{-4}
37	0.15	0.87	6.83	4.13×10^{-4}
40	0.17	0.84	8.64	3.06×10^{-4}
50	0.20	0.79	8.98	1.81×10^{-4}
60	0.41	0.58	27.32	1.20×10^{-4}
70	0.43	0.58	29.70	9.45×10^{-5}
80	0.46	0.54	30.06	5.30×10^{-5}
100	0.63	0.38	33.72	1.25×10^{-4}

[a] Here χ^2 is the mean-squared error of the fitting.

%, the trans-to-cis photoisomerization rate shows a slight decrease. When the water content varies in a range from 23 to 37 vol %, the trans-to-cis photoisomerization rate does not show a detectable variation. When the water content increases from 37 to 50 vol %, the trans-to-cis isomerization rate decreases gradually, which results from the cluster collapse due to the hydrophobic interaction. When the water content increases from 50 to 60 vol %, a dramatic decrease of the photoisomerization rate can be observed. As indicated in section 3.5, H-aggregation occurs at the water content of 60 vol %. When the water content further increases to 80%, the trans-to-cis isomerization rate shows a slight decrease. Finally, when the water content approaches about 100% (i.e., THF in the microphase is almost completely replaced by H_2O), the isomerization rate significantly decreases again due to the structure "freeze" and chain entanglement.

The study on the trans-to-cis isomerization degree at the photostationary state gives the same structure variation information. The isomerization degree at the photostationary state is estimated from

$$\text{isomerization degree} = (A_{origin} - A_s)/A_{origin} \qquad (9)$$

where A_{origin} is the absorbance at λ_{max} before the light irradiation and A_s is the absorbance at the same wavelength measured at the photostationary state. Figure 13b shows the isomerization degree of $POAPB_6P$-AC solutions or dispersions varying with the water content. There is a sudden drop of the isomerization degree when the water content increases from 50 to 60 vol %. When THF in the microphase is almost completely replaced by H_2O, the isomerization degree shows another sudden drop.

The result obtained from the photoisomerization study is consistent with the results discussed in the other parts of this paper. It strongly suggests that the colloid formation undergoes several different stages in the stepwise buildup process as the water content increases. For the system discussed above, when the water content reaches 23%, the $POAPB_6P$-AC chains start to associate, which is accompanied by the slight decrease of the photoisomerization rate and the isomerization degree. When the water content increases from 23 to 37 vol %, more and more polymer chains transfer from the "isolated" single-chains to the associated chains, which is indicated by the cluster size increase (Figure 5). At this stage, the structures formed in the dispersions are loose and can be disrupted by the UV light irradiation, which is a result of the volume expansion and hydrophilicity increase caused by the trans-to-cis isomerization.[1,41] As a result, the observed photoisomerization rate and isomerization degree do not show an obvious variation. When the water content increases from 37 to 60 vol %, the loose clusters of associated chains undergo a collapse, which is indicated by the significant cluster size contraction. When the water content varies in a range from 50 to 60 vol %, the photoisomerization rate and isomerization degree significantly decrease because of the hindrance of the closely packed polymer chains. Another important factor causing such variation is the formation of H-aggregates when the water content reaches 60 vol %. The H-aggregation can also strongly hinder the isomerization, as pointed out by many authors previously.[25,26,32] Finally, when THF in the microphase is almost completely replaced by H_2O, the colloidal structure is completely "frozen" due to the free volume decrease and chain entanglement, which again causes the obvious decrease in the isomerization rate and degree. The spectral blue shift appearing in this stage (Figure 11) is also related with the structure variation in the microphase.

The above results clearly show that H-aggregation can be formed only when polymer chains are closely packed after the cluster collapse, but at the same time, the chromophore motion has not been completely "frozen" by the free volume decrease and chain entanglement. The specific water contents for H-aggregate formation and other microphase transitions should depend on the factors such as chemical structure of the chain units, degree of functionalization, molecular weight and distribution, and initial concentration of the polymer in the organic solvent, among others. Although this paper has no attempt to give a full picture of those correlations, it is believed that the results obtained in this paper can supply some basic understanding of colloidal sphere formation and its relationship with H-aggregation in the system. On the basis of the understanding, the inner structure of the colloidal spheres can be controlled by adjusting the preparation conditions.

4. Summary

An amphiphilic random copolymer functionalized with branched azo side chains, $POAPB_6P$-AC, has been synthesized

and used to investigate the H-aggregation and the colloidal sphere formation through the gradual hydrophobic association in the mixed aqueous−organic media. Results indicate that the microphase transition and structure formation are closely related with the water content in the systems. The polymeric chains start to associate at the critical water content (CWC). CWC is dependent on the initial concentration of the polymer in the THF solution and is estimated to be 23 vol % when the initial concentration is 1.0 mg/mL. When the water content reaches 37%, the fraction of associated chains in the dispersion is estimated to be 99.5%. When the water content increases from 37 to 60 vol %, the clusters of associated chains undergo a collapse. When the water content reaches about 60%, azo chromophores of $POAPB_6P$-AC start to form H-aggregates, as indicated by the significant blue shift from 360 to 339 nm in the UV−vis spectra. Meanwhile, the dominant structures in the system transform from clusters to colloidal spheres after the collapse. When THF in the microphase is almost completely replaced by H_2O, the colloidal structure is completely "frozen" due to the free volume decrease and chain entanglement, which is indicated by an obvious decrease of the isomerization rate and degree. For the first time, the results indicate that in colloidal sphere formation process the H-aggregation can occur only at a specific stage, at which the azo chromophores are closely packed, but their movements have not been completely restricted by the surrounding chains.

Acknowledgment. The financial support from the NSFC under Projects 50533040 and 20374033 is gratefully acknowledged.

Supporting Information Available: Scheme for synthesis of $OAPB_6P$ and $POAPB_6P$-AC; analytical data and spectra of products of each step reaction for $OAPB_6P$ synthesis. This material is available free of charge via the Internet at http://pubs.acs.org.

References and Notes

(1) Kumar, G. S.; Nechers, D. C. *Chem. Rev.* **1989**, *89*, 1915.
(2) Xie, S.; Natansohn, A.; Rochon, P. *Chem. Mater.* **1993**, *5*, 403.
(3) Delaire, J. A.; Nakatani, K. *Chem. Rev.* **2000**, *100*, 1817.
(4) Natansohn, A.; Rochon, P. *Chem. Rev.* **2002**, *102*, 4139.
(5) Ikeda, T.; Horiuchi, S.; Karanjit, D. B.; Kurihara, S.; Tazuke, S. *Macromolecules* **1990**, *23*, 36.
(6) Todorov, T.; Nikolova, L.; Tomova, N. *Appl. Opt.* **1984**, *23*, 4309.
(7) Rochon, P.; Batalla, E.; Natansohn, A. *Appl. Phys. Lett.* **1995**, *66*, 136.
(8) Kim, D. Y.; Tripathy, S. K.; Li, L.; Kumar, J. *Appl. Phys. Lett.* **1995**, *66*, 1166.
(9) Finkelmann, H.; Nishikawa, E.; Pereira, G. G.; Warmer, M. *Phys. Rev. Lett.* **2001**, *87*, 015501.
(10) Li, M. H.; Keller, P.; Li, B.; Wang, X. G.; Brunet, M. *Adv. Mater.* **2003**, *15*, 569.
(11) Yu, Y. L.; Nakano, M.; Ikeda, T. *Nature (London)* **2003**, *425*, 145.
(12) Nikolova, L.; Todorov, T.; Ivanov, M.; Andruzzi, F.; Hvilsted, S.; Ramanujam, P. S. *Opt. Mater.* **1997**, *8*, 255.
(13) Lee, S.-H.; Kumar, J.; Tripathy, S. K. *Langmuir* **2000**, *16*, 10482.
(14) Ichimura, K.; Oh, S. K.; Nakagawa, M. *Science* **2000**, *288*, 1624.
(15) Lvov, Y.; Yamada, S.; Kunitake, T. *Thin Solid Films* **1997**, *300*, 107.
(16) Wang, X.; Balasubramanian, S.; Li, L.; Jiang, X.; Sandman, D. J.; Rubner, M. F.; Kumar, J.; Tripathy, S. K. *Macromol. Rapid Commun.* **1997**, *18*, 451.
(17) Laschewsky, A.; Wischerhoff, E.; Kauranen, M.; Persoons, A. *Macromolecules* **1997**, *30*, 8304.
(18) Wang, X. G.; Balasubramanian, S.; Kumar, J.; Tripathy, S. K.; Li, L. *Chem. Mater.* **1998**, *10*, 1546.
(19) Dante, S.; Advincula, R.; Frank, C. W.; Stroeve, P. *Langmuir* **1999**, *15*, 193.
(20) Wu, L. F.; Tuo, X. L.; Cheng, H.; Chen, Z.; Wang, X. G. *Macromolecules* **2001**, *34*, 8005.
(21) Wang, G.; Tong, X.; Zhao, Y. *Macromolecules* **2004**, *37*, 8911.
(22) Decher, G.; Hong, J. D.; Schmitt, J. *Thin Solid Films* **1992**, *210/211*, 831.
(23) Halperin, A.; Tirrell, M.; Lodge, T. P. *Adv. Polym. Sci.* **1992**, *100*, 31.
(24) Steed, J. W.; Atwood, J. L. *Supramolecular Chemistry*; John Wiley & Sons Ltd.: New York, 2000; p 26.
(25) Sturmer, D. W.; Heseltine, D. W. In James, T. H., Ed.; *The Theory of the Photographic Process*; Macmillan Publishing Co. Inc.: New York, 1977; p 194.
(26) Herz, A. H. *Photogr. Sci. Eng.* **1974**, *18*, 323.
(27) (a) McRae, E. G.; Kasha, M. *J. Chem. Phys.* **1958**, *28*, 721. (b) Philpott, M. R.; Lee, J. W. *J. Chem. Phys.* **1972**, *57*, 2026.
(28) Vekshin, N. L. *J. Photochem. Photobiol., B* **1989**, *3*, 625.
(29) See, for example: (a) Monahan, A. R.; Blossey, D. F. *J. Phys. Chem.* **1970**, *74*, 4014. (b) Monahan, A. R.; Germano, J. J.; Blossey, D. F. *J. Phys. Chem.* **1971**, *75*, 1227.
(30) See, for example: (a) Tinoco, I. *J. Am. Chem. Soc.* **1960**, *82*, 4785. (b) Bolton, H. C.; Weiss, J. J. *Nature (London)* **1962**, *195*, 666.
(31) See, for example: (a) Spano, F. C.; Mukamel, S. *J. Chem. Phys.* **1989**, *91*, 683. (b) Yang, Y. *J. Opt. Soc. Am. B* **1991**, *8*, 981. (c) Misawa, K.; Ono, H.; Minoshima, K.; Kobayashi, T. *Appl. Phys. Lett.* **1993**, *63*, 577. (d) Grad, J.; Hernandez, S.; Mukamel, S. *Phys. Rev. A* **1988**, *37*, 3835. (e) Steinhoff, R.; Chi, L. F.; Marowsky, G.; Mobius, D. *J. Opt. Soc. Am. B* **1989**, *6*, 843.
(32) See, for example: (a) Kunitake, T. *Angew. Chem., Int. Ed. Engl.* **1992**, *31*, 709. (b) Anzai, J.-I.; Osa, T. *Tetrahedron* **1994**, *50*, 4039. (c) Whitten, D. G.; Chen, L. H.; Geiger, H. C.; Perlstein, J.; Song, X. S. *J. Phys. Chem. B* **1998**, *102*, 10098. (d) Kinoshita, T. *J. Photochem. Photobiol., B* **1998**, *42*, 12. (e) Pedrosa, J.-M.; Romero, M. T. M.; Camacho, L.; Mobius, D. *J. Phys. Chem. B* **2002**, *106*, 2583.
(33) Song, X. S.; Perlstein, J.; Whitten, D. G. *J. Am. Chem. Soc.* **1997**, *119*, 9144.
(34) (a) Hayashita, T.; Kurosawa, T.; Miyata, T.; Tanaka, K.; Igawa, M. *Colloid Polym. Sci.* **1994**, *272*, 1611. (b) Yang, L.; Takisawa, N.; Hayashita, T.; Shirahama, K. *J. Phys. Chem.* **1995**, *99*, 879. (c) Kang, H.-C.; Lee, B. M.; Yoon, J.; Yoon, M. *J. Colloid Interface Sci.* **2000**, *231*, 255.
(35) See, for example: (a) Saremi, F.; Tieke, B. *Adv. Mater.* **1998**, *10*, 388. (b) Hong, J. D.; Park, E. S.; Park, A. L. *Langmuir* **1999**, *15*, 6515. (c) Hong, J. D.; Jung, B. D.; Kim, C. H.; Kim, K. *Macromolecules* **2000**, *33*, 7905.
(36) Li, Y. B.; He, Y. N.; Tong, X. L.; Wang, X. G. *J. Am. Chem. Soc.* **2005**, *127*, 2402.
(37) Li, Y. B.; Deng, Y. H.; He, Y. N.; Tong, X. L.; Wang, X. G. *Langmuir* **2005**, *21*, 6567.
(38) Li, Y. B.; Tong, X. L.; He, Y. N.; Wang, X. G. *J. Am. Chem. Soc.* **2006**, *128*, 2220.
(39) Li, Y. B.; Deng, Y. H.; Tong, X. L.; Wang, X. G. *Macromolecules* **2006**, *39*, 1108.
(40) Wang, H. P.; He, Y. N.; Tuo, X. L.; Wang, X. G. *Macromolecules* **2004**, *37*, 135.
(41) Rau, H. *Photochemistry and Photophysics*; Rabek, J. F., Ed.; CRC Press: Boca Raton, FL, 1990; Vol. II, Chapter 4.
(42) Wu, L. F.; Tuo, X. L.; Cheng, H.; Chen, Z.; Wang, X. G. *Macromolecules* **2001**, *34*, 8005.
(43) (a) Zhang, L. F.; Shen, H. W.; Eisenberg, A. *Macromolecules* **1997**, *30*, 1001. (b) Shen, H. W.; Zhang, L. F.; Eisenberg, A. *J. Phys. Chem. B* **1997**, *101*, 4697.
(44) (a) Koppel, D. E. *J. Chem. Phys.* **1972**, *57*, 4814. (b) Berne, B.; Pecora, R. *Dynamic Light Scattering*; Plenum Press: New York, 1976.
(45) Chu, B. *Laser Light Scattering*; Academic Press: New York, 1991.
(46) Burchard, W. *Makromol. Chem., Macromol. Symp.* **1988**, *18*, 1.
(47) Ma, Y. H.; Cao, T.; Webber, S. E. *Macromolecules* **1998**, *31*, 1773.
(48) Liu, S. Y.; Hu, T. J.; Liang, H. J.; Jiang, M.; Wu, C. *Macromolecules* **2000**, *33*, 8640.
(49) Antonietti, M.; Heinz, S.; Schmidt, M.; Rosenauer, C. *Macromolecules* **1994**, *27*, 3276.

MA061335P